

**Original article:**

**SELENOPROTEIN M IS EXPRESSED DURING  
BONE DEVELOPMENT**

Melanie Grosch<sup>1</sup>, Jennifer Fuchs<sup>1</sup>, Michael Bösl<sup>2</sup>, Andreas Winterpacht<sup>1\*</sup>, Andreas Tagariello<sup>1</sup>

<sup>1</sup> Institute of Human Genetics, University Hospital Erlangen, University of Erlangen-Nürnberg, Erlangen, Germany

<sup>2</sup> Max Planck Institute of Neurobiology, Martinsried, Germany

\* corresponding author: Prof. Dr. A. Winterpacht, Institute of Human Genetics, University Hospital Erlangen, Friedrich-Alexander-University Erlangen-Nürnberg, Schwabachanlage 10, D-91054 Erlangen, Germany; Tel. ++49-9131-852-2019; FAX: ++49-9131-852-3232; E-mail: Andreas.Winterpacht@uk-erlangen.de

**ABSTRACT**

25 selenoproteins that contain selenium, incorporated as selenocysteine (Sec), have been identified to date. Selenoprotein M (SELM) is one of seven endoplasmic reticulum (ER)-resident, Sec-containing proteins that may be involved in posttranslational processing of proteins and maintenance of ER function. Since *SELM* was overrepresented in a cartilage- and bone-specific expressed sequence tag (EST) library, we further investigated the expression pattern of *Selm* and its possible biological function in the skeleton. RNA *in situ* hybridization of *Selm* in chicken and mice of different developmental stages revealed prominent expression in bones, specifically in osteoblast, and in tendons. This result suggests that SELM functions during bone development, where it is possibly involved in the processing of secreted proteins.

**Keywords:** selenium, selenoproteins, Kashin-Beck osteoarthropathy, bone development, thiol-disulfide oxidoreductase, unfolded protein response

**INTRODUCTION**

Selenium is an essential trace element that plays an important role in several metabolic pathways, including thyroid hormone metabolism, antioxidant defense system, and intracellular redox homeostasis (Gromer et al., 2005). Moreover, selenium has been shown to be incorporated as selenocysteine (Sec) into at least 25 human and 24 rodent selenoproteins identified so far (Behne and Kyriakopoulos, 2001; Kryukov et al., 2003; Reeves and Hoffmann, 2009). Sec is encoded by the UGA codon, and recognition of this 21<sup>st</sup> amino acid is ensured by a stem-loop structure in the 3' UTR termed the Sec insertion sequence (SECIS) (Driscoll and Copeland, 2003).

Although their precise biological functions remain unknown, recent data suggest that endoplasmic reticulum (ER)-resident selenoproteins form an important part of the ER quality control machinery (Labunskyy et al., 2007) and may be involved in the formation or isomerization of disulfide bonds and in the unfolded protein response (UPR) (Hawkes and Alkan, 2010). The correct folding of proteins is essential for ER function and plays a fundamental role in the secretory pathway. Accumulation of misfolded or unfolded proteins in the ER results in ER stress, which leads to translational attenuation, transcriptional activation of chaperones, and protein degradation (Schroder and Kaufman, 2005).

Selenoproteins are crucial for embryogenesis as targeted deletion of the Sec tRNA gene, *Trsp*, which is responsible for the expression of all selenoproteins, is embryonic lethal (Downey et al., 2009). Furthermore, *Col2a1* promoter-driven conditional knockout in osteochondroprogenitor cells revealed essential functions of selenoproteins in bone development. This corresponds to observations suggesting that bone tissue in man and rat is affected by selenium deficiency (Tsukahara et al., 1996; Moreno-Reyes et al., 2001). Moreover, selenium deficiency may also play a role in Kashin-Beck osteoarthropathy, endemic in China and Tibet (Moreno-Reyes et al., 1998).

SELM is an ER-resident selenoprotein that is predicted to function as a thiol-disulfide oxidoreductase (Ferguson et al., 2006). It contains a thioredoxin-like fold and a conserved CxxU active-site motif, which is characteristic of enzymes involved in the regulation of redox processes (Martin, 1995). We recently carried out an expressed sequence tag (EST) project to identify genes and pathways involved in skeletal development. As a result, we observed that *Selm* was overrepresented in human growth plate tissue (Tagariello et al., 2005). However, although SELM is thought to be involved in oxidative stress (Hwang et al., 2008; Yim et al., 2009; Garcia-Triana et al., 2010) and Alzheimer's disease (Hwang et al., 2005), the expression pattern and tissue-specific function of *Selm* remain unknown.

In the present study, we describe for the first time prominent *Selm* expression in bony structures and tendons of the developing chicken and mouse. The present data suggest that SELM may play a role in the proper folding and processing of secreted proteins during bone development.

## RESULTS AND DISCUSSION

We first analyzed the expression pattern of *SELM* by RNA *in situ* hybridization. Due

to an easier handling and better availability (especially of early stages), tissue sections of chicken wings aged 6 days (Hamburger Hamilton stage 29; HH29) to 14 days (HH40) were used (Figure 1A). At HH29 we observed *SELM* expression in the condensed mesenchyme that will develop into bone. In later developmental stages prominent expression in bones could be detected. This could be verified by detailed comparative analysis of serial sections of wings HH40 with different markers (Figure 1B, C). The *SELM* expression pattern largely coincides with that of osteocalcin (*BGLAP*) and also with alkaline phosphatase (AP), two markers for osteoblasts (Ducy and Karsenty, 1995; Schinke and Karsenty, 1999; Franz-Odenaal et al., 2006). These results suggest expression in osteoblasts. To exclude expression in chondrocytes and verify expression in osteoblasts, we carried out a semiquantitative PCR with cDNA of different cell types (Figure 2). In chicken micromass cultures, differentiated to chondrocytes for seven days, no *SELM* expression could be detected (Figure 2A). The chondrocyte phenotype was verified by type II (*COL2A1*) and type X (*COL10A1*) collagen, two markers for chondrocytes (Lefebvre and Smits 2005). In contrast, expression of *selm* could be detected in primary osteoblasts prepared from chicken calvariae and differentiated for 21 days (Figure 2B). Also in the murine pre-osteoblastic cell line MC3T3 (differentiated for 30 days) *Selm* could be detected together with the osteoblast markers Osteocalcin (*BGLAP*) and type I collagen (*COL1A1*) (Figure 2C).

Additional to expression in osteoblasts, we also observed expression in tendons. By RNA *in situ* hybridization of wings of different developmental stages we detected coexpression of *SELM*, scleraxis (*SCX*), and tenomodulin (*TNMD*) (Figures 3, 4). Since *SCX* and *TNMD* are specifically expressed in tenocytes (Blitz et al., 2009), our results demonstrate expression of *SELM* in this cell type.

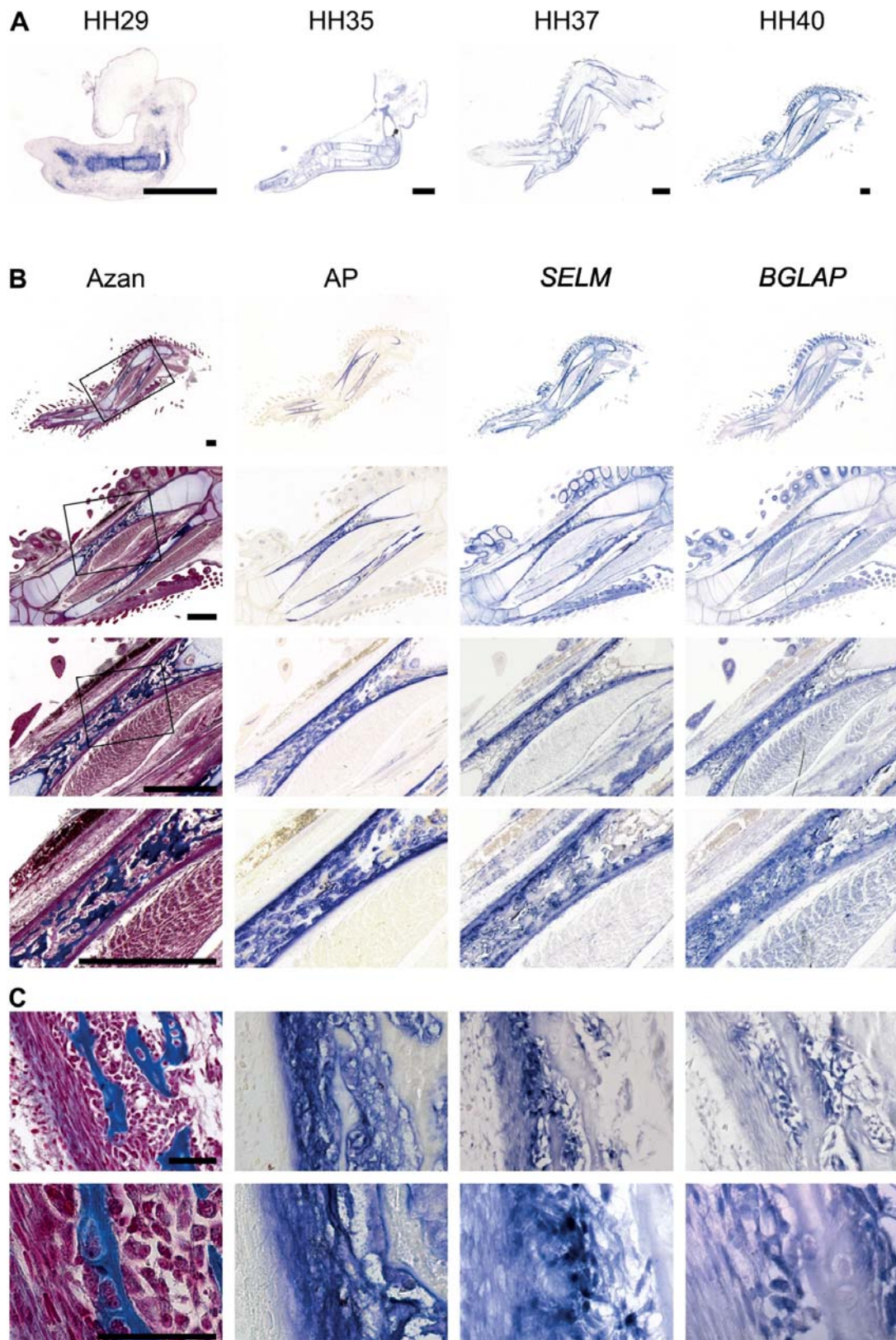


**Figure 1: SELM expression in long bones during chicken development**

RNA *in situ* hybridization on 5  $\mu$ m thick paraffin sections of wings of indicated developmental stages (A) and wings at stage HH40 (B).

(A) Sections were hybridized with antisense riboprobes against SELM. Scale bar, 1 mm.

(B, C) Serial sections were hybridized with antisense riboprobes against SELM and BGLAP, an additional Azan and alkaline phosphatase (AP) staining is shown. Scale bar, 1 mm (B), 50  $\mu$ m (C).

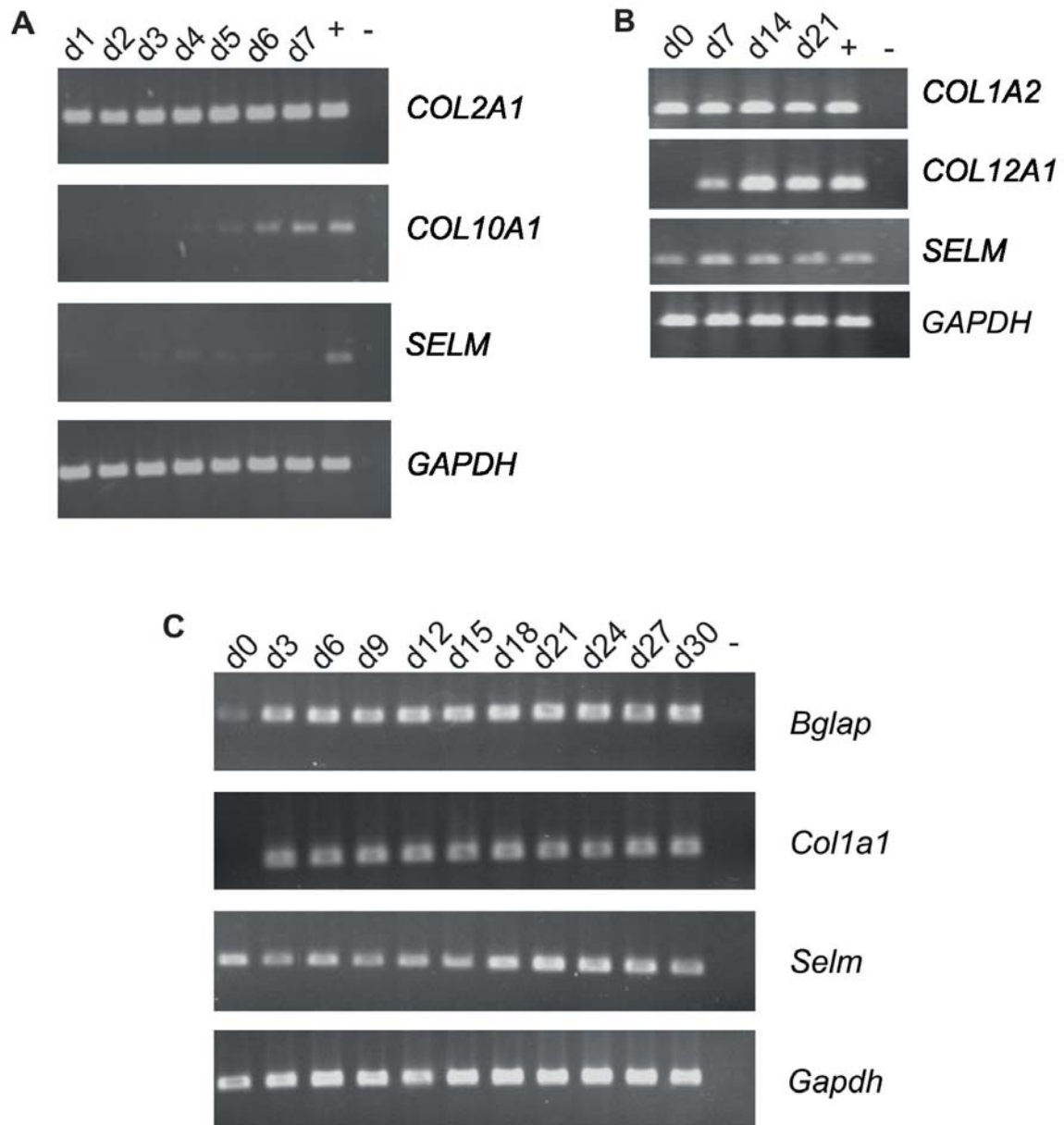


**Figure 2: *SELM* expression in osteoblasts**

Semiquantitative RT-PCR analysis of *SELM* expression in chicken micromass cultures (A), primary osteoblasts prepared from chicken calvariae HH41 (B) and in the murine pre-osteoblast cell line MC3T3 (C). Additional genes (as indicated) were used to verify the cell type, *Gapdh* served as loading control.



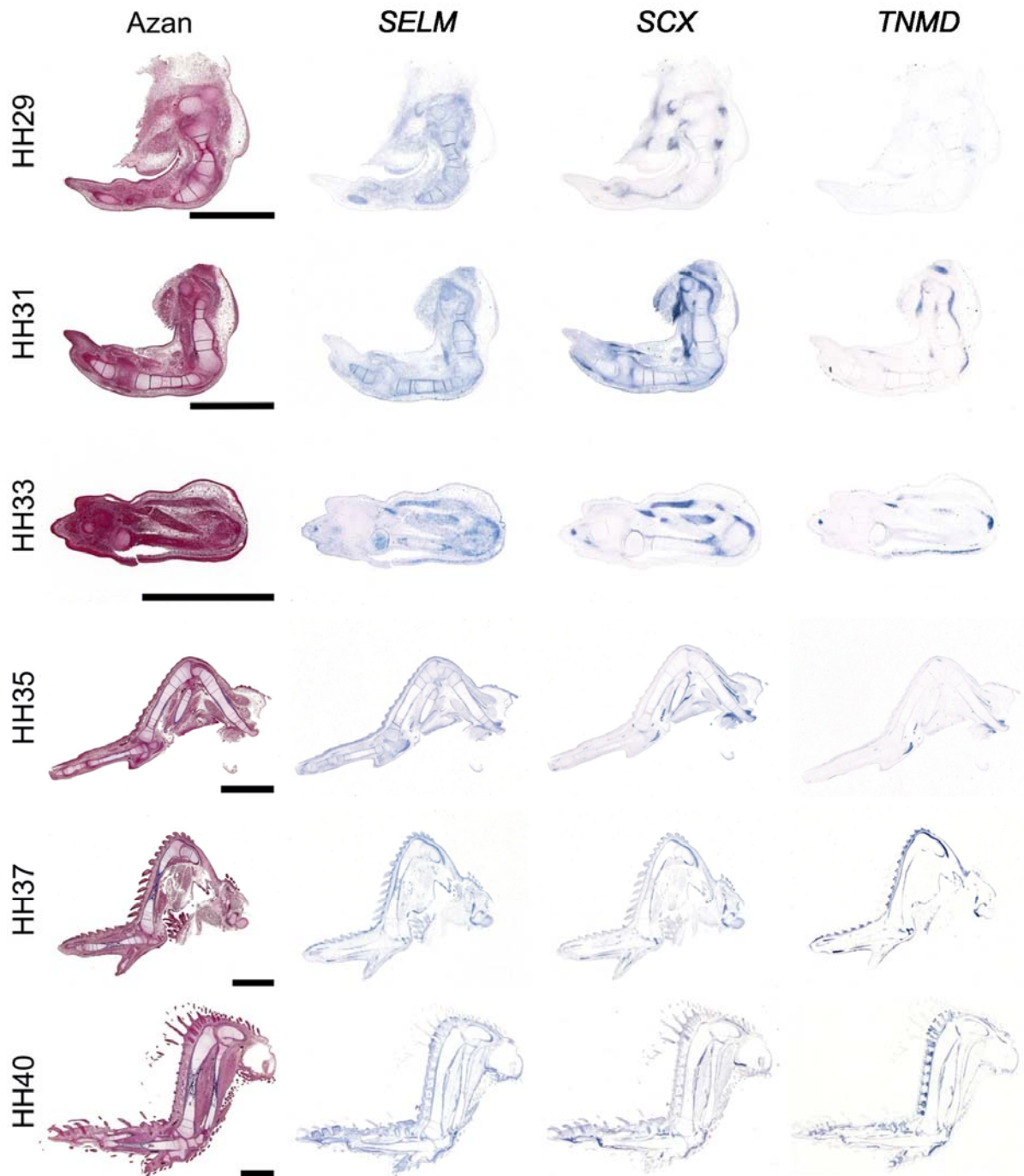


**Figure 3: Expression of *SELM* in tendons during chicken development**

RNA *in situ* hybridization on 5  $\mu$ m thick paraffin sections of wings of indicated developmental stages. Serial sections were hybridized with antisense riboprobes against *SELM*, *SCX* and *TNMD*, an additional Azan staining is shown. Scale bar, 2 mm.

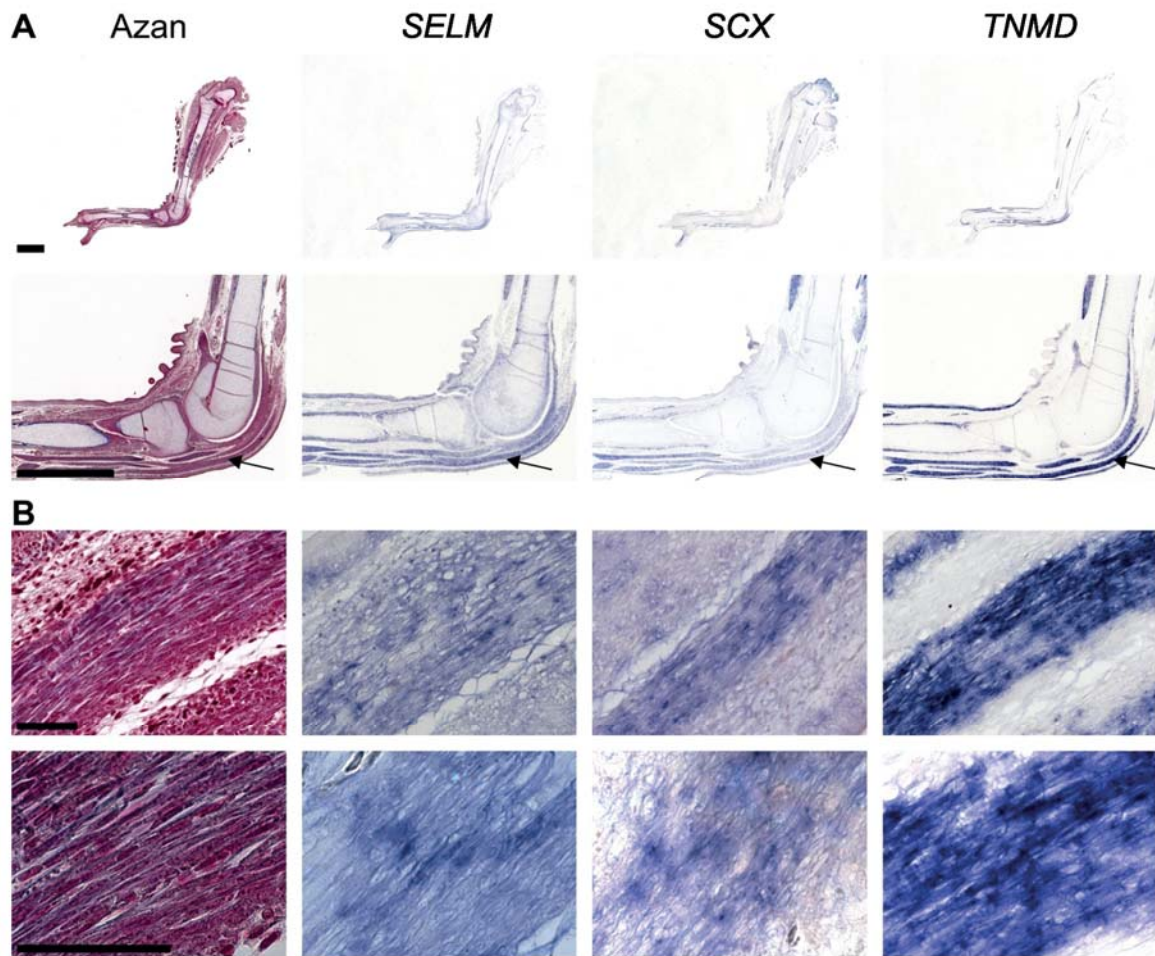


**Figure 4: *SELM* expression in tenocytes**

RNA *in situ* hybridization on 5  $\mu$ m thick paraffin sections of legs at stage HH38. Serial sections were hybridized with antisense riboprobes against *SELM*, *SCX* and *TNMD*, an additional Azan staining is shown. One tendon is marked by an arrow. Scale bar, 2 mm (A), 50  $\mu$ m (B).

To verify and further support the strong expression pattern of *SELM* especially in the developing bone we used another species and subsequently analyzed *Selm* expression on murine tissue sections by RNA *in situ* hybridization. On embryonic day E16.5, *Selm* was prominently expressed in the bones of the craniofacial, axial, and appendicular skeleton (Figure 5). In particular, expression in the vertebrae, maxilla, and mandibula could be detected (Figure 5A) as well as in the trabecular bone and the periosteum of long bones (Figure 5B and data not shown). This expression pattern largely coincides with that of *Bglap* (Figure 5A). In addition, we also observed expression of *Selm* in the olfactory epitheli-

um at this developmental stage (Figure 5A). We subsequently analyzed expression of *Selm* in the head and limb sections of 4-day-old mice (P4) (Figure 6). Strong expression of *Selm* was detected in the cerebellum and olfactory epithelium, and to a lesser extent in the hippocampus (Figure 6A). These results corroborate the recent findings of a study by Zhang et al. (2008), which demonstrated elevated *Selm* expression in the cerebellum, olfactory bulb, Ammon's horn, and hippocampus. We found additional expression in the teeth and bones that resembled the expression pattern of *Bglap* (Figure 6A). Moreover, expression of *Selm* was observed in the periosteum and trabecular bone of P4 hindlimb sections



(Figure 6B). Comparison of the expression pattern of *Selm* with that of markers for early (*Colla1*) and late (*Bglap*) osteoblasts (Jikko et al., 1999; Cohen, 2006; Kulterer et al., 2007), revealed overall coexpression of

*Selm* and *Colla1*. In contrast, coexpression of *Selm* and *Bglap* was restricted to the periosteum (Figure 6B).

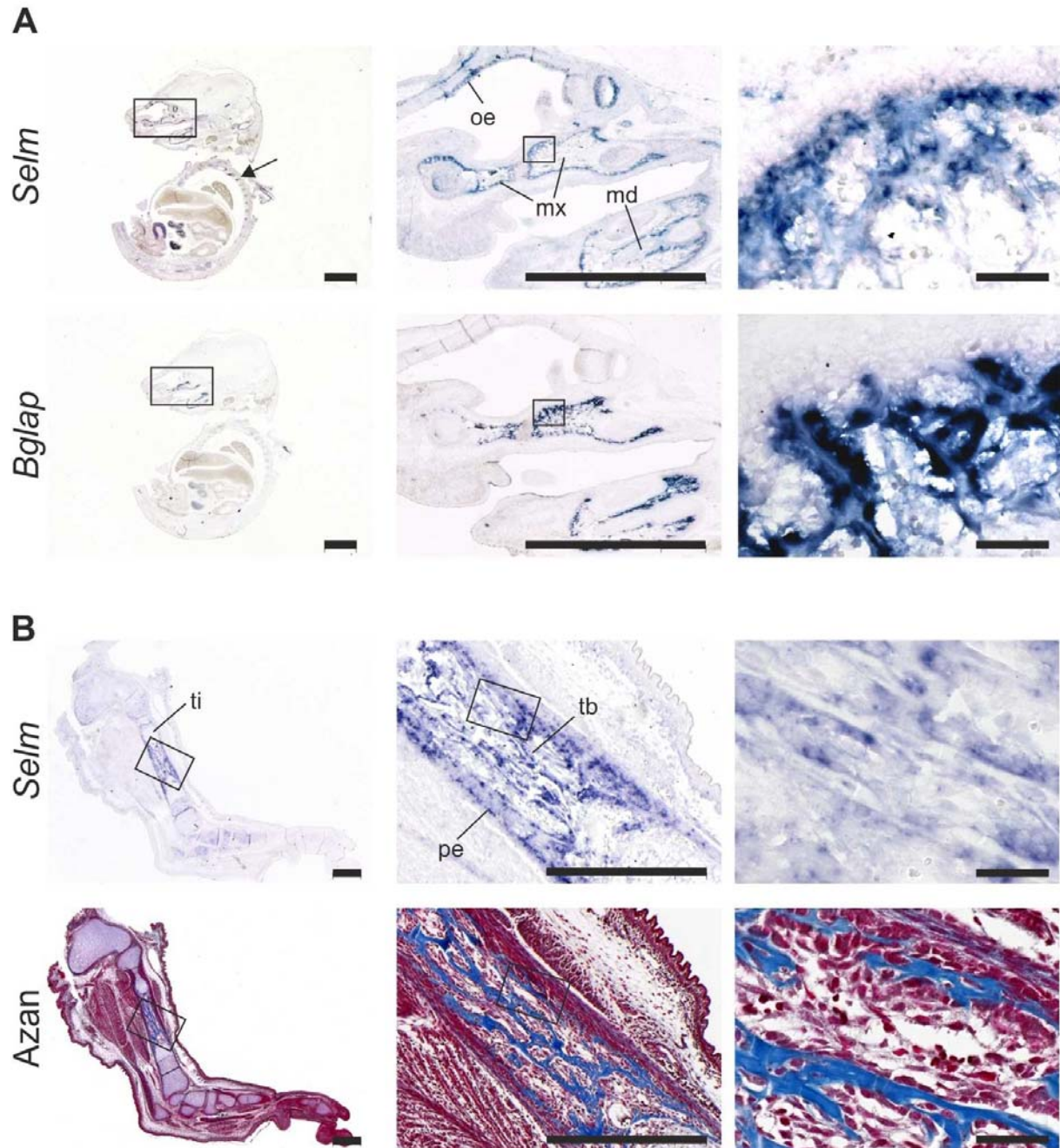


#### Figure 5: Expression of *Selm* in fetal mice (E16.5)

RNA *in situ* hybridization on 5  $\mu$ m thick paraffin sections of whole embryos (A) and hindlimbs (B). Scale bar, 2 mm.

(A) Sections were hybridized with antisense riboprobes against *Selm* and *Bglap* as indicated. Vertebrae are marked by an arrow. md, mandibula; mx, maxilla; oe, olfactory epithelium.

(B) Sections were hybridized with antisense riboprobes against *Selm*, an additional Azan staining is shown. Pe, periosteum; tb, trabecular bone; ti, tibia.

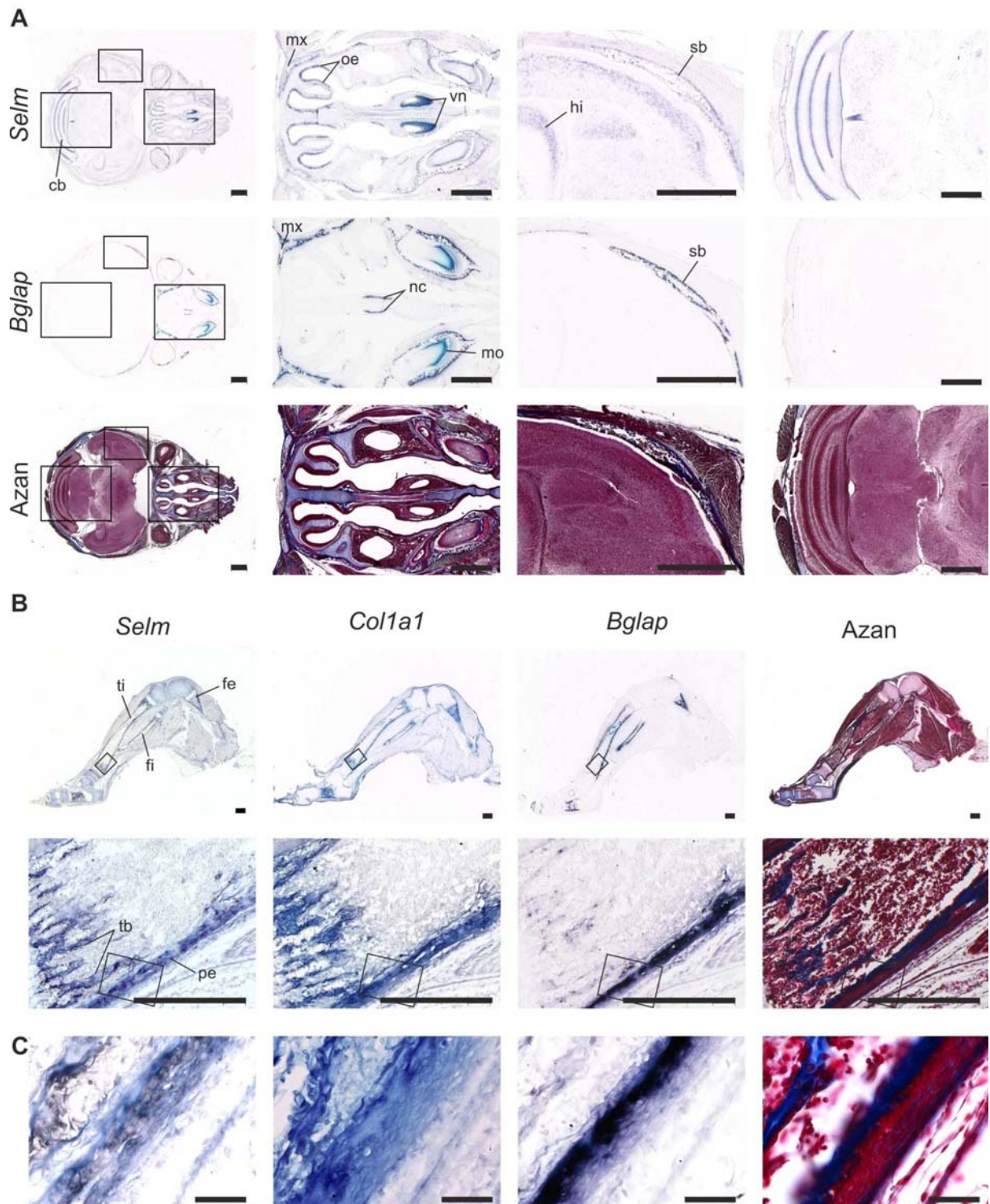


### Figure 6: Expression of *Selm* in juvenile mice (P4)

RNA *in situ* hybridization on 5 µm thick paraffin serial sections of the head of postnatal day 4 (P4) mice (**A**; scale bar, 1 mm) and hindlimbs (**B**; scale bar, 0.5 mm). Sections were hybridized with anti-sense riboprobes against *Selm*, *Bglap*, and *Col1a1*, and stained with Azan as indicated. (**C**) Magnified views of the corresponding boxed areas in **B**. cb, cerebellum; fe, femur; fi, fibula; hi, hippocampus; mo, molar; mx, maxilla; nc, nasal concha; oe, olfactory epithelium; sb, sphenoid bone; tb, trabecular bone, ti, tibia; pe, periosteum; vn, vomeronasal organ.



Since strong *Selm* expression was observed in osteoblasts during bone development, we aimed to elucidate potential functions of SELM in osteoblasts *in vivo*. We generated a mutant mouse strain from ES cells (C57BL/6) containing a genetic deletion of *Selm* (*Selm*<sup>-/-</sup>; [Supplementary Figure 1](#)). The open reading frame (ORF) of *Selm* in these ES cells was replaced with a ZEN-Ub1 cassette that contains a *LacZ* reporter gene under transcriptional control of the endogenous gene promoter. Although complete loss of *Selm* expression was verified by RNA *in situ* hybridization and real-time PCR ([Supplementary Figure 1](#)), *Selm* deficiency did not affect viability or fertility.

Moreover, morphological and histological analyses did not reveal any visible skeletal abnormalities, indicating that *Selm* deficiency may be compensated by other selenoproteins. Nevertheless, we used the *Selm*<sup>-/-</sup> mice to verify the expression pattern of *Selm* by X-Gal staining of E16.5 (Figure 7A) and P4 (Figure 7B) mice, which express  $\beta$ -galactosidase under the control of the *Selm* promoter ([Supplementary Figure 1](#)). As shown in Figure 7A (e, f) comparative Alizarin red and Alcian blue staining for visualization of bone and cartilage, respectively, confirmed expression of *Selm* in almost all bony structures of the skeleton.

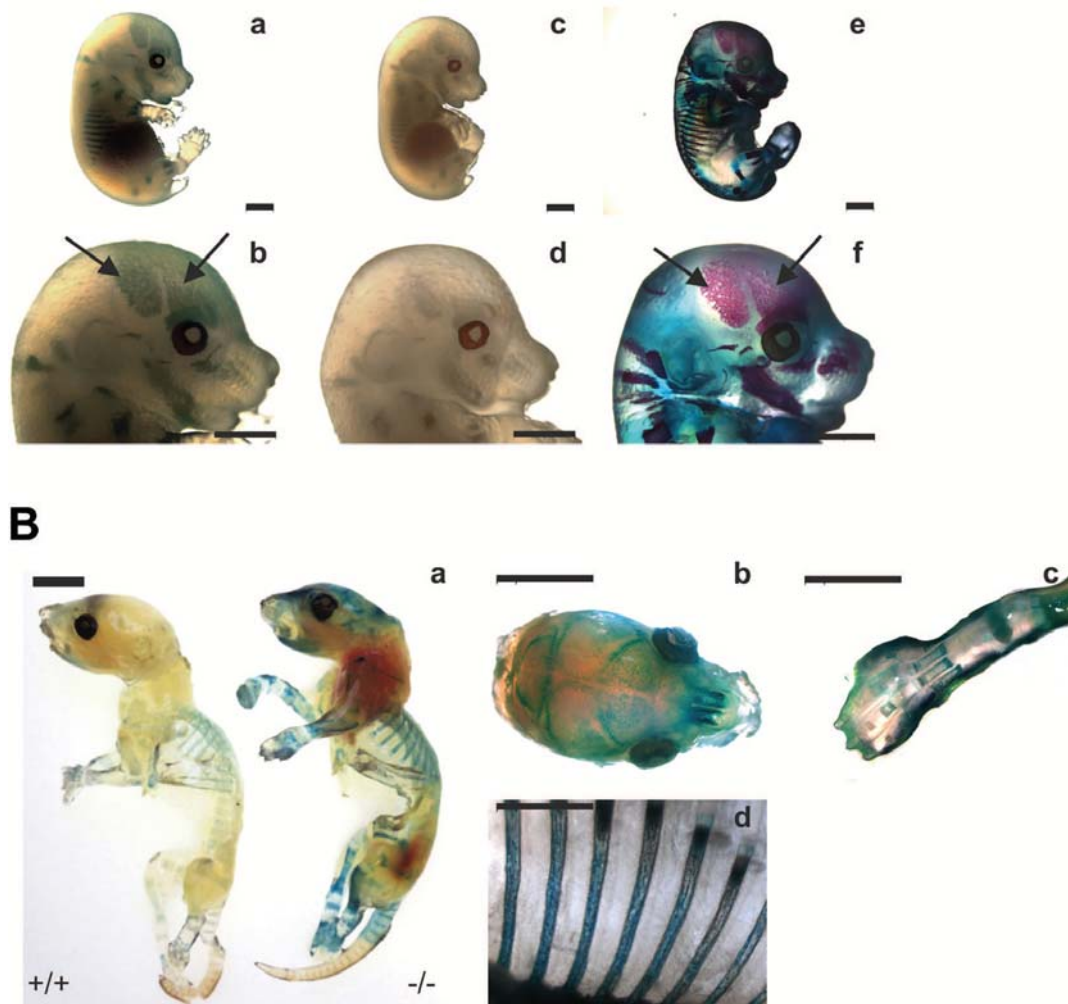


**Figure 7: X-Gal staining**

(A) X-Gal staining of E16.5 *Selm*<sup>-/-</sup> (a, b) and wild type mice (c, d). Wild type embryos were simultaneously stained with Alizarin red and Alcian blue to visualize bone and cartilage, respectively (e, f). Calvarial bones are marked by arrows. Scale bar, 2 mm.

(B) X-Gal staining of P4 wild type (+/+) and *Selm*<sup>-/-</sup> mice (-/-). Staining of the head (b), hindlimb (c), and ribs (d) of *Selm*<sup>-/-</sup> mice is shown in detail. Scale bar, 5 mm.

The present study is the first to analyze *SELM* expression in chicken and mouse sections during development and to link *SELM* with bone and tendon development. The ER-localized *SELM* protein possesses (1) a thioredoxin-like domain, (2) a surface-accessible active-site redox motif, and (3) structural similarities to other characterized thiol-disulfide oxidoreductases (Korotkov et al., 2002), suggesting that *SELM* represents a thiol-disulfide isomerase that is involved in disulfide bond formation in the ER (Ferguson et al., 2006). Moreover, the high expression level of *SELM* in osteoblasts and tenocytes — the main matrix producing cells of bones and tendons, respectively — indicates that *SELM* plays a role in the processing of ECM proteins. The ER is the site of synthesis and processing of secretory pathway proteins, which include transmembrane proteins and constituents of the extracellular matrix. In osteoblasts and tenocytes, vast amounts of ECM proteins, particularly the fibrillar collagens COL1A1 and COL1A2, are synthesized and secreted. Correct folding is a prerequisite for exiting the ER, whereas misfolded proteins are retained. Accumulation of misfolded or underglycosylated proteins results in ER stress — a process that has been shown to play a fundamental role in the initiation and progression of a wide range of connective tissue disorders (Boot-Handford and Briggs 2010). Together with observations demonstrating an involvement of *SELM* in unfolded protein response (UPR) and ER stress (Grosch et al., unpublished), the data indicate that *SELM* may play a role in the proper folding and processing of secreted proteins during bone and tendon development.

## EXPERIMENTAL PROCEDURES

### *Ethics statement*

All mouse experiments were approved by the Ethics Committee for Animal Experiments of the University of Erlangen (TS-05/10).

### *RNA in situ hybridization*

RNA *in situ* hybridization on 5 µm paraffin sections of chicken or mouse tissue using digoxigenin-labeled antisense riboprobes for *Selm*, *Coll1a1*, and *Bglap* was carried out as previously reported (Schmidl et al., 2006). Specific cDNA fragments for murine *Selm* (NM\_053267) and *Bglap* (NM\_001032298) antisense riboprobes were obtained by RT-PCR

- (*Selm*, 5'-ttcttcagcccttggctcc-3' and 5'-acttgcggtagaagccgagc-3');
- *Bglap*, 5'-catgaggaccctctctctgc-3' and 5'-tgccagagtttggcttagg-3') and cloned into pCRII-TOPO and pCR4-TOPO vectors, respectively. Specific cDNA fragments for chicken *SELM*, *BGLAP* (NM\_205387), *SCX* (NM\_204253) and *TNMD* (NM\_206985) antisense riboprobes were obtained by RT-PCR
- (*SELM*, 5'-gcggtgggtgacggctgagccgg-3' and 5'-ttacaggtctgggtgctctcttg-3');
- *BGLAP*, 5'-gctcacattcagcctctgc-3' and 5'-ggagaagtggagcataatgg-3');
- *SCX*, 5'-agctgtccaagatcgagacg-3' and 5'-gtgaagacgggagtgtgtcc-3');
- *TNMD*, 5'-accttcaggagtgggaacg-3' and 5'-tccgtgtagtcgttgacagg-3') and cloned into the pCR4-TOPO vector. The *Coll1a1* plasmid was a kind gift from Dr. Michael Stock.

### *Cell culture*

The pre-osteoblast murine cell line MC3T3 (ATCC) was cultivated in alpha modified Eagle's medium supplemented with 10 % FCS and 100 U/ml penicillin/streptomycin at 37 °C and 5 % CO<sub>2</sub>. Cells were differentiated for 30 days by adding of 50 mg/ml ascorbic acid and 50 mg/ml glycerol-2-phosphate to the culture medium.

### *Micromass cultures*

Micromass cultures were prepared from chicken limb buds (HH22-24) by digestion with 3 mg/ml dispase followed by treatment with 0.1 % collagenase Ia and 0.1 % trypsin. Cells were cultivated in DMEM:F-12 (1:1) supplemented with 10 % FCS, 0.2 % CS and 100 U/ml penicillin/streptomycin at

37 °C and 5 % CO<sub>2</sub>. Culture medium was changed every day.

### Primary osteoblasts

Primary osteoblasts were prepared from the calvariae of chicken (HH41). Chicken calvariae were digested with 1,5 U/ml collagenase P and 0,05 % trypsin.

Primary osteoblasts were cultivated in alpha modified Eagle's medium supplemented with 10 % fetal calf serum (FCS) and 100 U/ml penicillin/streptomycin in 6-well plates at 37 °C and 5 % CO<sub>2</sub>. The culture medium was changed every 3 days. When the cells reached confluency, they were differentiated for 21 days by adding of 50 mg/ml ascorbic acid and 50 mg/ml glycerol-2-phosphate to the culture medium.

### RT-PCR

Total RNA was isolated from cells using TRIzol (Invitrogen). First-strand cDNA was synthesized with oligo(dT) primer and Superscript III Reverse Transcriptase (Invitrogen), according to manufacturer's instructions.

To verify the osteoblast or chondrocyte phenotype of cell cultures, semiquantitative RT-PCR with following primers was carried out

- (*COL1A2*, 5'-gcaacattggattccctggacc-3' and 5'-gttcacccttttctccctgcc-3');
- *COL2A1*, 5'-ccaacaccgccagcatcc-3' and 5'-gccaatatccacgccaactcct-3');
- *COL10A1*, 5'-gccaatatccacgccaactcct-3' and 5'-cagaggaatagagaccat-3');
- *COL12A1*, 5'-gcagaacaaacctctact-3' and 5'-ttcttggtgtctctctcc-3');
- *SELM*, 5'-gcggtgggtgacggctgagccgg-3' and 5'-ttacaggtctgggtggtccttcttg-3');
- *Bglap*, 5'-catgaggacctctctctgc-3' and 5'-tgccagagtttgcttagg-3');
- *Colla1*, 5'-cctgtaaaagatggtgcc-3' and 5'-caccaggttcaccttgcacc-3');
- *Selm*, 5'-ttcttgacgccctgtggctcc-3' and 5'-actgcggtagaagccgagc-3');
- *Gapdh* was used as control (*GAPDH*, 5'-gtggagtccactggtgtcttc-3' and 5'-atcagcagcctcactac-3');

- *Gapdh*, 5'-gtggagtccactggtgtcttc-3' and 5'-ctccgacgcctgcttcaccac-3').

### Alcian blue and Alizarin red staining

Whole E15.5 embryos or skinned and eviscerated P4 mice were fixed in 95 % EtOH for 1–2 days. Mice were moved into glass vials and immersed in acetone overnight at room temperature. Subsequently, mice were rinsed in 95 % EtOH and stained for cartilage in Alcian blue (0.015 % Alcian blue 8GX, 76 % EtOH, and 20 % glacial acid). After washing with 95 % EtOH overnight and clearing in 1 % KOH (embryo) or 2 % KOH (P4), mice were stained in 0.005 % Alizarin red S in 1 % KOH for 3 to 6 h. For clearing of stained mice, samples were incubated in 5 % KOH for 5 days followed by a series of clearing solutions containing increasing glycerol and decreasing KOH concentrations (80:20, 60:40, 40:60, 20:80; 1 % KOH:glycerol). Finally, samples were stored in 100 % glycerol.

### X-Gal staining

Whole E15.5 embryos or skinned and eviscerated P4 mice were fixed in 4 % paraformaldehyde for 1 h at 4°C. After 3 washing steps in pre-washing solution (1× PBS and 2 mM MgCl<sub>2</sub>) at 4°C, samples were incubated twice for 15 min at room temperature (RT) in detergent solution (1× PBS, 2 mM MgCl<sub>2</sub>, 0.02 % NP-40, and 0.01 % Na-deoxycholate) before incubation at RT with staining solution (1× PBS, 20 mM Tris-HCl [pH 7.5], 2 mM MgCl<sub>2</sub>, 0.02 % NP-40, 0.01 % Na-deoxycholate, 5 mM K<sub>3</sub>Fe(CN)<sub>6</sub>, 5 mM K<sub>4</sub>Fe(CN)<sub>6</sub>, and 0.75 mg/ml X-Gal in DMSO) under visual observation. Subsequently, samples were washed 3 times in post-washing solution (1× PBS and 5 mM EDTA, pH 8) and post-fixed overnight at 4°C in 4 % paraformaldehyde. For clearing of X-Gal stained mice, samples were incubated in 5 % KOH for 5 days followed by a series of clearing solutions containing increasing glycerol and decreasing KOH concentrations (80:20, 60:40, 40:60, 20:80; 1 % KOH:glycerol).



Finally, samples were stored in 100 % glycerol.

### ACKNOWLEDGMENTS

We would like to thank Dr. Michael Stock for providing the *Coll1a1* plasmid.

### REFERENCES

- Behne D, Kyriakopoulos A. Mammalian selenium-containing proteins. *Annu Rev Nutr* 2001;21:453-73.
- Blitz E, Viukov S, Sharir A, Shwartz Y, Galloway JL, Pryce BA et al. Bone ridge patterning during musculoskeletal assembly is mediated through SCX regulation of Bmp4 at the tendon-skeleton junction. *Dev Cell* 2009;17:861-73.
- Boot-Handford RP, Briggs MD. The unfolded protein response and its relevance to connective tissue diseases. *Cell Tissue Res* 2010;339:197-211.
- Cohen MM, Jr. The new bone biology: pathologic, molecular, and clinical correlates. *Am J Med Genet A* 2006;140:2646-706.
- Downey CM, Horton CR, Carlson BA, Parsons TE, Hatfield DL, Hallgrimsson B et al. Osteo-chondroprogenitor-specific deletion of the selenocysteine tRNA gene, *Trsp*, leads to chondronecrosis and abnormal skeletal development: a putative model for Kashin-Beck disease. *PLoS Genet* 2009;5:e1000616.
- Driscoll DM, Copeland PR. Mechanism and regulation of selenoprotein synthesis. *Annu Rev Nutr* 2003;23:17-40.
- Ducy P, Karsenty G. Two distinct osteoblast-specific cis-acting elements control expression of a mouse osteocalcin gene. *Mol Cell Biol* 1995;15:1858-69.
- Ferguson AD, Labunskyy VM, Fomenko DE, Arac D, Chelliah Y, Amezcua CA et al. NMR structures of the selenoproteins Sep15 and SelM reveal redox activity of a new thioredoxin-like family. *J Biol Chem* 2006;281:3536-43.
- Franz-Odenaal TA, Hall BK, Witten PE. Buried alive: how osteoblasts become osteocytes. *Dev Dyn* 2006;235:176-90.
- Garcia-Triana A, Gomez-Jimenez S, Peregrino-Uriarte AB, Lopez-Zavala A, Gonzalez-Aguilar G, Sotelo-Mundo RR et al. Expression and silencing of Selenoprotein M (SelM) from the white shrimp *Litopenaeus vannamei*: effect on peroxidase activity and hydrogen peroxide concentration in gills and hepatopancreas. *Comp Biochem Physiol A* 2010;155:200-4.
- Gromer S, Eubel JK, Lee BL, Jacob J. Human selenoproteins at a glance. *Cell Mol Life Sci* 2005;62:2414-37.
- Hawkes WC, Alkan Z. Regulation of redox signaling by selenoproteins. *Biol Trace Elem Res* 2010;134:235-51.
- Hwang DY, Cho JS, Oh JH, Shim SB, Jee SW, Lee SH et al. Differentially expressed genes in transgenic mice carrying human mutant presenilin-2 (N141I): correlation of selenoprotein M with Alzheimer's disease. *Neurochem Res* 2005;30:1009-19.
- Hwang DY, Sin JS, Kim MS, Yim SY, Kim YK, Kim CK et al. Overexpression of human selenoprotein M differentially regulates the concentrations of antioxidants and H<sub>2</sub>O<sub>2</sub>, the activity of antioxidant enzymes, and the composition of white blood cells in a transgenic rat. *Int J Mol Med* 2008;21:169-79.
- Jikko A, Harris SE, Chen D, Mendrick DL, Damsky CH. Collagen integrin receptors regulate early osteoblast differentiation induced by BMP-2. *J Bone Miner Res* 1999;14:1075-83.

Korotkov KV, Novoselov SV, Hatfield DL, Gladyshev VN. Mammalian selenoprotein in which selenocysteine (Sec) incorporation is supported by a new form of Sec insertion sequence element. *Mol Cell Biol* 2002;22:1402-11.

Kryukov GV, Castellano S, Novoselov SV, Lobanov AV, Zehtab O, Guigo R et al. Characterization of mammalian selenoproteomes. *Science* 2003;300:1439-43.

Kulterer B, Friedl G, Jandrositz A, Sanchez-Cabo F, Prokesch A, Paar C et al. Gene expression profiling of human mesenchymal stem cells derived from bone marrow during expansion and osteoblast differentiation. *BMC Genomics* 2007;8:70.

Labunskyy VM, Hatfield DL, Gladyshev VN. The Sep15 protein family: roles in disulfide bond formation and quality control in the endoplasmic reticulum. *IUBMB Life* 2007;59:1-5.

Lefebvre V, Smits P. Transcriptional control of chondrocyte fate and differentiation. *Birth Defects Res C Embryo Today* 2005;75:200-12.

Martin JL. Thioredoxin - a fold for all reasons. *Structure* 1995;3:245-50.

Moreno-Reyes R, Suetens C, Mathieu F, Begaux F, Zhu D, Rivera MT et al. Kashin-Beck osteoarthropathy in rural Tibet in relation to selenium and iodine status. *N Engl J Med* 1998;339:1112-20.

Moreno-Reyes R, Egrise D, Neve J, Pasteels JL, Schoutens A. Selenium deficiency-induced growth retardation is associated with an impaired bone metabolism and osteopenia. *J Bone Miner Res* 2001;16:1556-63.

Reeves MA, Hoffmann PR. The human selenoproteome: recent insights into functions and regulation. *Cell Mol Life Sci* 2009;66:2457-2478.

Schinke T, Karsenty G. Characterization of Osfl, an osteoblast-specific transcription factor binding to a critical cis-acting element in the mouse Osteocalcin promoters. *J Biol Chem* 1999;274:30182-9.

Schmidl M, Adam N, Surmann-Schmitt C, Hattori T, Stock M, Dietz U et al. Twisted gastrulation modulates bone morphogenetic protein-induced collagen II and X expression in chondrocytes in vitro and in vivo. *J Biol Chem* 2006;281:31790-800.

Schroder M, Kaufman RJ. The mammalian unfolded protein response. *Annu Rev Biochem* 2005;74:739-89.

Tagariello A, Schlaubitz S, Hankeln T, Mohrmann G, Stelzer C, Schweizer A et al. Expression profiling of human fetal growth plate cartilage by EST sequencing. *Matrix Biology* 2005;24:530-8.

Tsukahara H, Deguchi Y, Miura M, Hata K, Hori C, Hiraoka M et al. Selenium status and skeletal tissue metabolism in young infants. *Eur J Pediatr* 1996;155:148-9.

Yim SY, Chae KR, Shim SB, Hong JT, Park JY, Lee CY et al. ERK activation induced by selenium treatment significantly downregulates beta/gamma-secretase activity and Tau phosphorylation in the transgenic rat overexpressing human selenoprotein M. *Int J Mol Med* 2009;24:91-6.

Zhang Y, Zhou Y, Schweizer U, Savaskan NE, Hua D, Kipnis J et al. Comparative analysis of selenocysteine machinery and selenoproteome gene expression in mouse brain identifies neurons as key functional sites of selenium in mammals. *J Biol Chem* 2008;283:2427-38.